Published in final edited form as:
Methods. 2014 October 1; 69(3): 315–325. doi:10.1016/j.ymeth.2014.06.003.

Integrative analysis of independent transcriptome data for rare diseases

Zhe Zhang[a], **Zeyad Hailat**[b], **Marni J. Falk**[c], and **Xue–wen Chen**[b,1]

[a]Center for Biomedical Informatics, Children's Hospital of Philadelphia, Philadelphia PA, USA 19104

[b]Department of Computer Science, Wayne State University, 5057 Woodward Avenue, Suite 3010, Detroit, MI, USA 48202

[c]Division of Human Genetics, The Children's Hospital of Philadelphia and University of Pennsylvania Perelman School of Medicine, Philadelphia, PA, USA 19104

Abstract

High–throughput technologies used to interrogate transcriptomes have been generating a great amount of publicly available gene expression data. For raw diseases that lack of clinical samples and research funding, there is a practical benefit to jointly analyze existing datasets commonly related to a specific rare disease. In this study, we collected a number of independently generated transcriptome data sets from four species: Human, Fly, Mouse and Worm. All data sets included samples with both normal and abnormal mitochondrial functions. We reprocessed each data set to standardize format, scale and gene annotation and used HomoloGene database to map genes between species. Standard procedure was also applied to compare gene expression profiles of normal and abnormal mitochondrial functions to identify differentially expressed genes. We further used meta–analysis and other integrative analyses to recognize patterns across data sets and species. Novel insights related to mitochondrial dysfunctions was revealed via these analyses, such as a group of genes consistently dysregulated by impaired mitochondrial function in multiple species. This study created a template for the study of rare diseases using genomic technologies and advanced statistical methods. All data and results generated by this study are freely available and stored at http://goo.gl/nOGWC2, to support further data mining.

Keywords

transcriptome data; mitochondrial dysfunction; integrative analysis

1. Introduction

The study of rare disease is limited by the availability of samples and other resources although it often helps researchers answer extremely important biomedical questions [1, 2, 3]. Some rare diseases can serve as models for more common one due to their close

[1]Tel: +1 (313) 577 – 2478, Fax: + 1 (313) 577 – 6868, xuewen.chen@wayne.edu (Xue–wen Chen).
zhangz@email.chop.edu (Zhe Zhang), zmhailat@wayne.edu (Zeyad Hailat), falkm@email.chop.edu (Marni J. Falk)

association. For example, primary mitochondrial diseases have a combined occurrence of about 1/5000 [4], but the investigation of these diseases have revealed extensive knowledge about mitochondrial dysfunction [5, 6], which has been commonly observed in diabetes [7], cancer [8] and neurodegenerative diseases [9, 10].

A deeper understanding of rare diseases can be achieved through utilization of innovative technologies, model animals, and integrative analysis of independently generated data sets. Paring modern genomic technologies with advanced statistical analysis has become an extremely valuable approach for investigating rare diseases [11, 12, 13]. This approach characterizes the overall state of one or more cellular systems, such as transcriptome, epigenome, and metabalome, and uses bioinformatic analysis to explore their interactions. It is then able to compensate for the small sample size of individual experiments with high dimension of data.

Integration of genomic data is practical challenging. Independently generated genomic data sets could be different from each other in many ways, such as technology, cell type, annotation, and data quality, which makes it critical to properly document metadata related to each experiment. Gene Expression Omnibus (GEO) [14], a public repository of transcriptome data sets, archives the metadata, raw data, and processed data of over 46, 000 data series. GEO provides an ideal platform for researchers to identify and access existing gene expression data sets related to a specific disease.

In this study, we present a semi–automated workflow to archive transcriptome data sets related to a specific rare disease, primary mitochondrial dysfunction. We have used this workflow to create Transcriptome of Mitochondrial Dysfunctions (ToMD), which currently includes 30 independent data sets and about 500 biological samples. Each of these data sets compared samples with primary mitochondrial dysfunction to those with normal or rescued mitochondrial function. Statistical methods were designed to evaluate data quality, standardize gene annotation, and perform integrative analysis. Preliminary analysis of these data sets has revealed new insights about primary mitochondrial diseases. All data sets and analysis results within archive are freely available http://goo.gl/nOGWC2.

2. Material and Methods

Below is a step-by-step description of the generation of ToMD. It is a semi-automated workflow that includes reproducible data processing and analysis steps, but also requires human decisions about data quality, sample grouping, analysis parameters, and so on.

2.1. Structure of the data archive

ToMD was structured in three tiers as described below:

1. Tier 1 is a collection of transcriptome data sets related to mitochondrial dysfunctions. It includes published data sets stored in GEO or other resources. All data sets were re-processed with a common procedure so they are properly normalized and annotated with unique ENTREZ gene IDs.

2. Tier 2 is a collection of results from pairwise comparisons. Each comparison was performed on two groups of samples within the same data set. Samples of one group usually have impaired mitochondrial functions induced by genetic or environmental factors while samples of the other group are controls with normal or rescued mitochondrial functions.

3. Tier 3 includes results of integrative analysis of data or results from multiple data sets. Given the high diversity of the data sets, each integrative analysis was customarily designed and documented in a separate subfolder. While it is unlikely to automate such analysis, we noticed that the availability of Tier 1 and 2 makes the integrative analysis much more efficient.

2.2. Identification of data sets

We worked closely with clinical researchers who treat mitochondrial diseases to search public repositories for transcriptome data sets related to primary mitochondrial diseases. These data sets were generated from human tissues and cell lines, as well as three model animals: C. elegans (worm), D. melanogaster (fruit fly), and M. musculus (mouse). No data generated from Sus scrofa (domestic pig) was selected due to the incompleteness of its gene annotation. Each data set includes two or more sample groups corresponding to abnormal and normal/rescued mitochondrial function. The mitochondrial dysfunction could be caused by pathogenic gene mutations in patients, knockdown/knockout of key mitochondrial genes in cultured cells or model animals, or exposure to chemicals such as Rotenone and Rapamycin.

Table 1 describes the four living species datasets. The table shows each dataset species, the dataset id that is used in this study, the dataset reference, the GEO id, the tissue, number of samples and genes, and the number of sample groups. The fly dataset compiles two different dataset sources with 12, 521 overlapped genes. The worm dataset compiles three different datasets with 16, 688 overlapped genes. The Human dataset compiles 13 different datasets with 895 overlapped genes then we excluded one of the human datasets because of too many missing values. The Mouse dataset compiles 12 different datasets with 10, 279 overlapped genes then we excluded one of the datasets because of too many missing values. Table 2 shows the four compiled species datasets, it shows the number of genes and samples for each species, in the *single* part of the table.

We used *HomoloGene* [45], a tool to build putative homology groups from the full genome of a different eukaryotic species, to construct putative orthologs for the four species. We used the putative orthologs to identified the species genes overlap in the constructed datasets as shown in table 2. Table 2 shows four groups of dataset information. The first part of the table shows the compiled datasets for each species under the heading single. The second part, *pairwise*; we constructed this group of datasets by identifying the overlapped genes in each pair of the species datasets. This group contains six subgroups of datasets. The third group of datasets comes from finding the overlap of three different species in one group. This group constructed from four different triplet combinations of the four species datasets.

The last group is identified as the overlap between the four species datasets where we find 235 overlapped genes under 445 different samples from the dataset.

2.3. Data processing

The processing of original data sets was done independently, so they often have different scale and gene annotation. It is then necessary to re-process all data sets to make them more consistent with each other. We applied two procedures to different types of data sets. For data sets generated on Affymetrix microarrays with their raw data files available, we directly processed the raw data using RMA method [46] and the custom library files provided by BRAINARRAY [47]. The output was a data matrix annotated with non-redundant Entrez gene IDs. For data sets not generated on Affymatrix microarrays or with no raw data available, we mapped the existing annotation to Entrez gene ID and collapsed redundant IDs by taking averages. Additionally, we made sure that all data sets were properly normalized and in log-2 scale. All samples were also re-labeled to replace original sample IDs with identifiers indicative of their mitochondrial function.

Data quality was evaluated based on criteria such as number of samples, percentage of missing values, sample-sample correlation. Data sets and samples with questionable quality would be excluded from statistical analysis.

2.4. Pairwise comparison of sample groups

We repetitively performed pairwise comparisons of two groups of samples with abnormal and normal/rescued mitochondrial functions. There could be more than one comparison per data set. For example, GEO series GEO1462 includes three subtypes of mitochondrial diseases and control samples, so the pairwise comparison was performed between the controls and each subtype. Another example is series GSE42986 that includes samples collected from both muscle biopsies and fibroblast cell lines, so the comparison was performed separately for two cell types.

The SAM (Significance Analysis of Microarrays) method was used for all pairwise comparisons to report the folder change, p value, and false discovery rate (FDR) to indicate the differential expression of each gene between two groups. We applied our in-house workflow to generate standard outputs for each pair-wise comparison. Within the outputs, there was a PDF report that summarizes the comparison with a set of statistics, tables and plots, such as the number of differentially expressed genes under given FDR cutoffs and a plot of principal components analysis (Figure 1). Another part of the outputs is an automatically generated Excel files with the complete results of SAM analysis and the functional annotation of differentially expressed genes by DAVID.

2.5. Integrative analysis

A major benefit of data sets archived in ToMD is the support to efficient integrative analysis. Not only integrative analysis increases the overall statistical power by combining samples from multiple studies, but also it systematically investigates multiple biological systems and will possibly reveal knowledge that cannot be discovered from a single study. We are performing a series of such analyses based on this platform, and the results of three finished analyses are now available as part of the tier 3 in ToMD.

The first two sets of results were generated by meta–analysis. One of them used the results of 60 normal vs. abnormal pairwise comparisons and the other was performed on the results of 12 patients vs. controls comparisons generated from 8 human data sets of different cell types and disease subtypes. Fisher's meta–analysis method [48] was used to calculate combined p values from p values from individual comparisons, and the goal was to identify genes consistently changing their expression level across comparisons.

The other analysis is an unsupervised biclustering of both samples and genes across data sets. The following sections will describe this analysis in detail.

2.6. Biclustering method

Clustering methods are used to group set of objects that shares specific features. Each group is called cluster. In the context of gene expression data under set of conditions (e.g., patients, time points), the cluster of genes is defined as a group of genes that falls in the same functional unit across the entire set of conditions in the dataset.

The process of clustering groups set of shared feature objects into groups based on only one dimension and cannot use any other dimensions simultaneously. Clustering methods aim to find groups of objects with high similarity among the same cluster members and increase the dissimilarity between different clusters.

Identifying a cluster of genes across all conditions assume similarity for all conditions which is not true in real world dataset for most cases because set of genes should be grouped based on subset of the conditions instead of all conditions.

Biclustering methods is first proposed by Cheng et al. [49] to find the biclusters in gene expression data. Biclustering methods goal is to identify biclusters that include subset of both dataset dimensions simultaneously. For example, in gene expression data where one dimension is genes list while the other is the set of samples. Biclustering methods aim to identify the subset of genes that are expressed under subset of samples simultaneously. As a result each bicluster includes a subset of genes and a subset of the samples.

In this section, we describe step-by-step procedure that we used to process and identify biclusters in each dataset.

2.6.1. Missing value recovery—The number of missing values is different across datasets. We used the R package *KNN impute* to identify and recover the missing values in each dataset. Two of the datasets have a large number of missing values that made it hared to recover, in one hand and in the other recovering this large amount of data will make a major change of the dataset that might not reflect the actual complexity of the dataset and affect the final results. The datasets are GSE24945 and GSE18677 with 9, 000 and 68, 000 of missing values; respectively. So we exclude them from this study.

In some datasets, some gene names were missing and hard to identify, in such cases we excluded these genes from the study. In some other cases, we have gene names duplication where the same gene occur more than once in the same dataset, we exclude the genes in such cases to eliminate any possible ambiguity in the dataset.

2.6.2. Re-normalization of data across datasets—Since the datasets come form different sources, we normalized them to the standard $z - score$ in column-wise where the column represent samples. The z score for each value in the column is calculating using the equation:

$$z = \frac{(x - \mu)}{\sigma}$$

where: x is the gene values in specific sample; μ is the column mean; and σ is the column standard deviation.

2.6.3. Mapping of gene annotation among the same species—For each species, we mapped the gene annotation of the species datasets, and then we merged them into one new dataset. The new dataset compiles the shared genes in the species datasets under all samples. This step identified four new datasets; a dataset for each species.

Table 2 shows that Worm dataset has the largest number of genes with 16, 688 across 42 samples. Human dataset has the largest number of samples compiles 233 with the smallest number of genes 895. Fly species has the smallest number of samples 33 with 12, 521 genes. Mouse dataset compiles 10, 279 genes across 147 samples.

2.6.4. Mapping of gene annotation among different species—We mapped the four species datasets that were constructed in the former step across each other to find the shared genes. The mapping included comparing the datasets in pairs, which result in identifying six new datasets, a new dataset for each pair of species. The new datasets are described in table 2. The number of shared genes across pairs of species are varies from 2, 944 shared genes between fly and mouse species datasets to 377 shared genes between human and worm species datasets.

We mapped the species dataset gene annotations in triplets. This process identified four different triplets datasets with 1, 637 genes across fly, worm and mouse to 286 across human, worm and mouse.

Mapping all of the species gene annotations results in 235 mapped genes across the four species with 445 different samples. Table 2 shows the mapping of gene annotation details.

We then processed the new datasets across the species to find the overlapped genes for each pair of species.

2.6.5. Biclustering method—Many biclustering methods are proposed in the literature for biclustering biological data. Ben-Dor et al. [50] proposed Order-Preserving Sub-Matrixes (OPSM) bicluster method for gene expression data. We used OPSM method for identifying the biclusters in the datasets. We chose OPSM for several reasons. One reason is that OPSM method proved promising results in the literature. Other reason is the availability of the method implementation.

The OPSM algorithm works as described in the following steps:

- T is a set of samples and g is a gene.
- The samples in T can be ordered so that the expression values are sorted in ascending order (suppose the values are all unique).
- Suppose a submatrix A contains genes G and samples T.
- A is a bicluster if there is an ordering (permutation) of T such that the expression values of all genes in G are sorted in ascending order.

2.6.6. Bicluster quality – Mean Squared Residue—Cheng et al. [49] proposed bicluster quality measure. The proposed measure finds the error in the bicluster expression values by calculating the difference between each expression value and both column and row means, with the bicluster mean. The proposed method is given by the following formula:

$$MSR\,(X)=\frac{1}{|I||J|}\sum_{i\in I,j\in J}\left(X_{ij}-X_{I_j}-X_{_{iJ}}+X_{_{IJ}}\right)^2$$

Where:

- X is bicluster with $|I|$ rows and $|J|$ columns;
- $MSR(X)$ is the error in the bicluster;
- X_{ij} is the value in row i and column j;
- $X_{_{iJ}}=\frac{\Sigma_{j\in J}X_{ij}}{|J|}$ is the row mean ;
- $X_{_{Ij}}=\frac{\Sigma_{i\in I}X_{ij}}{|I|}$ is the column mean;
- $X_{_{IJ}}=\frac{\Sigma_{j,j}X_{ij}}{|J||I|}$ the overall mean;

The smaller the value of $MSR(X)$ the better quality of the bicluster.

We modified the formula to find the coherence among the bicluster components to make it more readable by calculating it by the following formula:

$$MSR_x=1-MSR\,(X)$$

In the coherence, the closer the value of MSR_X to 1 is the better bicluster.

2.6.7. Software—OPSM has been implemented in Biclustering Analysis Toolbox (BicAT) [51] tool that we used to identify the biclusters from different datasets. BicAT is a JAVA-based tool that implements set of biclustering algorithms and tools for processing gene expression data. In addition to that we used *R language* to process, compile, analyze and plot the dataset and results.

2.6.8. Enrichment analysis—The bicluster of genes and samples assumes that the genes in the same bicluster shares common features and functionality for specific set of samples. We calculated the computational quality of the bicluster by calculating the MSR of its expression values. The computational quality measure is not enough to prove the relevance of the bicluster genes for the same group. We applied a enrichment analysis to find the biological significant of the bicluster genes and samples. The analysis test shows the related genes information.

Enrichment analysis is a computational process that decide whether an a priori defined set of genes shows statistically significant. We used for this purpose the Functional Annotation Tool from DAVID Bioinformatics Resources [52]. It is a web based tool that is used to identify the biological pathways and the enriched Gene-Ontology (GO) terms of the genes cluster. We will show the enrichment analysis result for the best biclusters MSR score, for each dataset, in section 3.

2.6.9. Statistical significant—We used Fisher's exact test to measures the statistical significant of the bicluster of genes. It finds how likely that the enrichment of a cluster, with genes from a particular category, is to some extent greater than what is expected by chance.

We used the Benjamini correction method to correct the enrichment p–values in order to control family-wide false discovery rate under certain rate (e.g. ≤ 0.05). Benjamini correction method is one of the multiple testing correction methods that is provided by DAVID tools.

The cluster p-value range from zero to one, the closer p-value to zero the more biological significant Since the p-value is for multiple test so we used the False Discovery Rate (FDR) adjusted p–value .

For each bicluster of genes, we applied the functional annotation tool to find the Gene Ontology (GO) terms, each subset genes from the bicluster has a GO term with a p–value that shows how significant is the list of genes. The GO term describes the set of genes and what they have in common.

3. Result

3.1. Meta-analysis of pairwise comparisons

We performed 60 pairwise comparisons to identify genes differentially expressed between sample groups of data sets. These comparisons included 12, 030 to 28, 360 unique genes (*mean* = 17, 410) and 4 to 22 biological samples (*mean* = 8.4). The outputs of each comparison were standardized, including a PDF report (Figure 1), statistical results of differential gene expression, and functional analysis of differentially expressed genes via DAVID. The statistical results of each gene include both fold change (magnitude) and statistical significance (p value and FDR) of group difference. Respectively 49 and 55 comparisons identified differentially expressed genes and enriched DAVID terms with *FDR* = 0.05. Therefore, sample groups of most comparisons do have different gene expression profiles. Table 3 listed some of the DAVID terms identified by 10 or more comparisons.

We then performed a meta–analysis of the comparison results. To compare genes of different species (worm, fly, mouse and human), gene IDs were mapped to homolog gene clusters based on HomoloGene database. Of totally 20, 441 homolog clusters, only 1, 241 were included in all 60 comparisons while respectively 18, 459 or 15, 333 clusters were included in at least 10 or 30 comparisons. The meta-analysis identified 12 gene clusters that were ranked top 2% of differential expression by at least 8 comparisons from at least 5 data sets and 3 species (Table 4). At least 9 of these genes encode proteins located in mitochondrion. For example, ETHE1 encodes a sulfur dioxygenase within mitochondrial matrix and its mutation causes ethylmalonic encephalopathy, a metabolic disorder.

Its differential expression was ranked top 2% by 12 comparisons of 7 data sets from all species. The conditions that caused differential expression of ETHE1 include: PGC-1a knockout in mouse muscle (decrease), knockdown of a cytochrome oxidase subunit in fly S2 cells (increase), treatment of worms with Rotenone (increase), muscle biopsy of MELAS patients (decrease), and so on.

Another analysis was performed on the results of pairwise comparisons to identify association between different conditions or treatments. It calculated the correlation coefficient between any two sets of fold changes of individual comparisons. Comparisons using the samples from the same data sets generally have stronger correlation to each other while significant correlation also exists between comparison results from different data sets and species (Table 5). For example, the overall transcriptomic changes in patient muscle biopsies were negatively correlated to the changes caused by treating human SK-N-MC cells with 50nM Rotenone for 4 weeks, but positively correlated to the changes caused by 5nM Rotenone for 1 week as well as Sirt3 knock out in mouse livers. Another example is the positive correlation between the changes caused by PGC-1alpha overexpression in mouse and Rotenone treatment in worm, two distantly related conditions.

3.2. Biclustering of genes and samples across datasets

In the genes and samples biclustering part of the study, after we prepared the datasets, we applied OPSM to extracted the biclusters from each dataset. After that we ranked them based on the bicluster MSR_X.

Some of the extracted biclusters includes hundreds of genes under small number of samples. In some other cases, some biclusters are including small number of genes with most of the samples. We filtered and excluded these two cases since they do not reflect a good quality clusters since one of the bicluster dimensions is very high and the other is very small.

Some cases, the number of genes or samples is less that 5. We excluded such cases from our results. Finally we included biclusters with gene counts and sample counts ≥ 5.

Table 2 summaries biclustering results for all species datasets and for all overlapped cases. In the sequel of this section we describe the biclustering results after filtering and measuring their quality.

3.2.1. Human dataset result—We identified and extracted biclusters from the human dataset and after filtering them we have 6 biclusters numbered from 3 to 8. Table 6 shows the extracted bicluster details. The highest MSR_X bicluster is bicluster 3 that includes 5 genes and 13 samples.

The enrichment analysis of human biclusters shows 100% genes enriched. Figure 2b shows bicluster 3 genes, samples and the bicluster plot that shows the relation between the genes and samples. Table 7 shows the enrichment analysis results for bicluster 3 using DAVID tool.

3.2.2. Mouse dataset result—We identified and extracted five biclusters from the mouse dataset after filtering. Table 8 shows the extracted bicluster details. Bicluster 3 has the highest MSR_X score. It includes 5 genes and 15 samples. Figure 3b shows bicluster 3 genes, samples and the bicluster plot that shows the genes, samples and the relation between them.

The enrichment analysis of bicluster 3 of mouse dataset shows that 40% of the genes are enriched. Bicluster 7 has the highest enrichment genes percent. The following genes are part of the extracted biclusters form the mouse dataset and none of them is enriched:

- Fgr, Wdr4, Allc, Icos, Pigu, Polr2a, Tat, Rab25, Cecr5, Dntt, Gtse1, Gstm3, Llgl2, Srrm1, Pih1d1, Tspo2, Rdh7

Table 8 describes mouse dataset biclusters details with enrichment analysis result.

3.2.3. Worm dataset result—We applied OPSM to the worm dataset. The method identified 6 different biclusters, after filtering, with different MSR_X scores. Bicluser 3 shows the highest MSR_X score; however, none of its genes were enriched. Bicluster 6 shows the highest enrichment gene percent. Table 9 shows the extracted bicluster details. Figure 4b shows bicluster 3 genes, samples and the bicluster plot that shows the correlation between the bicluster genes for the specified set of samples.

The following genes are part of the extracted biclusters form the worm dataset and none of them is enriched:

- C01G5.6, F54D10.5, B0464.9, sas-5, C13F10.7, C15H11.8, C18E3.9, K03H1.7, syn-16, C02F5.13, C48B4.11, Y57A10A.16, cpn-1, F18A1.8, ZK1248.11, cids-1, C39E9.12, D1007.8, T02C12.3, C04G6.4, C28A5.1, fbxa-210, F40F8.11, F49C12.9, F55A11.7, K06H6.2, lgg-3, T06D8.9, ZK1248.15, ztf-9, B0261.7, B0491.1, clec-127, C01G10.7, C01G8.1, C08F8.3, C14B1.2, C24D10.4, C42C1.12, C43E11.12, C43H8.2, F17A9.2, dhs-22, egg-2, fsn-1, F21D5.6, F41G3.6, F54A3.6, inx-22, K05C4.7, mvb-12, W01D2.5, pak-2, C35D10.10, Y54G11A.9, ZK1067.3

Table 9 shows worm dataset biclusters details with enrichment analysis results.

3.2.4. Fly dataset result—OPSM was able to extract, after filtering, 5 biclusters from fly dataset. The highest bicluster MSR_X score is bicluster 3. It involves 7 genes and 16 samples. Table 10 shows the extracted biclusters details.

Figure 5b shows bicluster 3 genes, samples and the bicluster plot that shows the bicluster genes, samples and the relation between them. Bicluster 3 shows the best enrichment percent.

The following genes are part of the extracted bicluster form fly dataset and none of them is enriched:

- CG2972, CG14270, CG11788, CG1749, sec13, CG10424, CG11875, CG13016, CG17249, CG18004, CG31223, mRpS23, CG32554, CG33213, CG3353, CG6617, CG7484, CG8090, Rae1, CG9947, CG12975, CG14286, CG6073

3.2.5. Different species mapping result—We mapped the four species gene annotations among the four species to find the overlapped genes among them. The overlapped datasets are falls in one of the following three categories based on the number of overlapped datasets:

1. Species pairs: In this category, we mapped the species datasets in pairs. Table 2 shows 6 overlapped pairs of datasets. The overlapped dataset of fly with worm result in 2, 724 genes across 75 samples produced highest number of biclusters 9 in this category. The biclusters extracted from this dataset shows the best average MSR_X results that means these bicluster are with high quality 0.96, that means the set of genes and samples in each bicluster share common features. The next best average biclusters quality is fly and mouse dataset with average MSR_X of 0.95. This show that fly dataset has common features with both worm and mouse datasets whereas the result biclusters of the fly and human overlap shows relatively small number of overlapped genes with average quality of biclusters. The overlapped dataset of human and worm shows smallest number of shared genes and the smallest average MSR_X. We extracted one bicluster form the mouse and human overlapped dataset, this bicluster was with MSR_X = 0.99; however, all of this bicluster samples are from mouse samples and the human samples are not included.

2. Species triplets: In this category, we mapped the species datasets three species at a time to find the overlapped genes. The result is four different datasets with 1, 637 overlapped genes between fly, mouse and worm. We extracted 7 biclusters from this dataset with average MSR_X of 0.92, three biclusters of them included samples from the three species and the other

four biclusters included samples from only two species. The other three overlapped datasets have an average of 300 overlapped genes among the species. The biclusters that extracted from these three datasets are of either number of genes less than 5 or number of samples less than 5 and they excluded from the list of biclusters.

3. All four species: The overlap among the four species produced a dataset of 235 genes and 445 samples, 7 biclusters extracted from this dataset with average $MRS_x = 0.85$. However, none of the extracted biclusters involved samples from all species. Three biclusters involved samples from human, fly and worm datasets. Two biclusters involved human and mouse dataset samples. One bicluster involoved human, fly and mouse and the last bicluster involved human fly and mouse samples.

4. Discussion

We developed a solution to overcome some of the difficulties in studying rare diseases. Genomic data sets seemingly divergent from each other, but commonly related to mitochondrial dysfunctions, were collected to generate a centralized platform of data mining, ToMD. Although many of the data processing and data analysis steps can be automated, we noticed that the key to the success of such a platform is the close control of data quality, sample grouping, and result interpretation by investigators with different domain knowledge.

Biclustering methods identify biclusters by involving both dimensions of dataset simultaneously, genes and samples in this study. Each bicluster includes a group of genes that falls in the same functional group under a subset of samples. We applied a robust biclustering method, OPSM, to identify co–regulated genes and samples across the different datasets. The method construct a bicluster if there is a permutation of the bicluster samples such that the expression values of the bicluster genes are sorted in ascending order.

Integrative analysis ToMD data sets have revealed new insights about mitochondrial diseases. For example, meta-analysis identified genes consistently having differential expression when mitochondrial functions were impaired across a variety of cell types and species. Follow-up study of the roles played by these genes in mitochondrial diseases will improve our understanding about these diseases and mitochondrial function in general.

The currents contents of ToMD are mostly static files. One of our future plans is to create a web interface that allows users to query, filter and analyze the data, as well as generate dynamic results and plots, which will further facilitate the process of knowledge discovery. Once the value of ToMD is further confirmed, we will apply the same principal to generate similar resources for other types of rare diseases, such as childhood cancers and congenital heart diseases.

5. Conclusion

In conclusion, we developed a practical strategy to reuse public data for the study of rare diseases whose low occurrence makes it difficult to collect large sample cohorts and obtain sufficient research funding. We proved that it is possible to integrate transcriptome data sets sharing a common link to a rare disease, but generated from different platforms, cell types, and even species.

Acknowledgments

The work was supported in part by US National Science Foundation award (IIS-0644366) to Xuewen Chen, and by the P30-HD026979 grant from the National Institute of Health. We thank Dr. Marni J. Falk for her help to identify data sets related to mitochondrial diseases.

References

[1]. Fishman MC. Author response to comment on “power of rare diseases: Found in translation”. Science translational medicine. 2014; 6(228):228lr1–228lr1.

[2]. van der Meer JW, Simon A, Dinarello CA. Comment on “power of rare diseases: Found in translation”. Science translational medicine. 2014; 6(219):219le1–219le1.

[3]. Fishman MC. Power of rare diseases: Found in translation. Science translational medicine. 2013; 5(201):201ps11–201ps11.

[4]. Schaefer AM, Taylor RW, Turnbull DM, Chinnery PF. The epidemiology of mitochondrial disorders—past, present and future. Biochimica et Biophysica Acta (BBA)-Bioenergetics. 2004; 1659(2):115–120. [PubMed: 15576042]

[5]. Rossignol R, et al. The expanding universe of mitochondrial research. The international journal of biochemistry & cell biology. 2013; 45(1):2–3. [PubMed: 23123864]

[6]. Wallace DC, et al. A mitochondrial bioenergetic etiology of disease. J Clin Invest. 123(4)

[7]. Dela F, Helge JW. Insulin resistance and mitochondrial function in skeletal muscle. The international journal of biochemistry & cell biology. 2013; 45(1):11–15. [PubMed: 23036788]

[8]. Iommarini L, Calvaruso MA, Kurelac I, Gasparre G, Porcelli AM. Complex i impairment in mitochondrial diseases and cancer: Parallel roads leading to different outcomes. The international journal of biochemistry & cell biology. 2013; 45(1):47–63. [PubMed: 22664328]

[9]. Oliveira J, Jekabsons MB, Chen S, Lin A, Rego AC, Gonçalves J, Ellerby LM, Nicholls DG. Mitochondrial dysfunction in huntington’s disease: the bioenergetics of isolated and in situ mitochondria from transgenic mice. Journal of neurochemistry. 2007; 101(1):241–249. [PubMed: 17394466]

[10]. Eckmann J, Eckert SH, Leuner K, Muller WE, Eckert GP. Mitochondria: mitochondrial membranes in brain ageing and neurodegeneration. The international journal of biochemistry & cell biology. 2013; 45(1):76–80. [PubMed: 22743330]

[11]. Zhang Z, Gasser DL, Rappaport EF, Falk MJ. Cross-platform expression microarray performance in a mouse model of mitochondrial disease therapy. Molecular genetics and metabolism. 2010; 99(3):309–318. [PubMed: 19944634]

[12]. Liu J, Zhang Z, Bando M, Itoh T, Deardorff MA, Clark D, Kaur M, Tandy S, Kondoh T, Rappaport E, et al. Transcriptional dysregulation in nipbl and cohesin mutant human cells. PLoS biology. 2009; 7(5):e1000119. [PubMed: 19468298]

[13]. Zhang Z, Chen D, Fenstermacher DA. Integrated analysis of independent gene expression microarray datasets improves the predictability of breast cancer outcome. BMC genomics. 2007; 8(1):331. [PubMed: 17883867]

[14]. Barrett T, Wilhite SE, Ledoux P, Evangelista C, Kim IF, Tomashevsky M, Marshall KA, Phillippy KH, Sherman PM, Holko M, et al. Ncbi geo: archive for functional genomics data sets—update. Nucleic acids research. 2013; 41(D1):D991–D995. [PubMed: 23193258]

[15]. Fernández-Ayala DJ, Chen S, Kemppainen E, MC O'Dell K, Jacobs HT. Gene expression in a drosophila model of mitochondrial disease. PLoS One. 2010; 5(1):e8549. [PubMed: 20066047]

[16]. Freije WA, Mandal S, Banerjee U. Expression profiling of attenuated mitochondrial function identifies retrograde signals in drosophila. G3: Genes— Genomes— Genetics. 2012; 2(8):843–851. [PubMed: 22908033]

[17]. Kayser E-B, Morgan PG, Hoppel CL, Sedensky MM. Mitochondrial expression and function of gas-1 in caenorhabditis elegans. Journal of Biological Chemistry. 2001; 276(23):20551–20558. [PubMed: 11278828]

[18]. Falk M, Zhang Z, Rosenjack J, Nissim I, Daikhin E, Nissim I, Sedensky M, Yudkoff M, Morgan P. Metabolic pathway profiling of mitochondrial respiratory chain mutants in¡ i¿ c. elegans¡/i¿. Molecular genetics and metabolism. 2008; 93(4):388–397. [PubMed: 18178500]

[19]. Schmeisser S, Priebe S, Groth M, Monajembashi S, Hemmerich P, Guthke R, Platzer M, Ristow M. Neuronal ros signaling rather than ampk/sirtuin-mediated energy sensing links dietary restriction to lifespan extension. Molecular metabolism. 2013; 2(2):92–102. [PubMed: 24199155]

[20]. Crimi M, Bordoni A, Menozzi G, Riva L, Fortunato F, Galbiati S, Del Bo R, Pozzoli U, Bresolin N, Comi GP. Skeletal muscle gene expression profiling in mitochondrial disorders. The FASEB journal. 2005; 19(7):866–868. [PubMed: 15728662]

[21]. Cížková A, Stráneckỳ V, Ivánek R, Hartmannová H, Nosková L, Piherová L, Tesařová M, Hansíková H, Honzík T, Zeman J, et al. Development of a human mitochondrial oligonucleotide microarray (h-mitoarray) and gene expression analysis of fibroblast cell lines from 13 patients with isolated f1fo atp synthase deficiency. BMC genomics. 2008; 9(1):38. [PubMed: 18221507]

[22]. Čížková A, Stráneckỳ V, Mayr JA, Tesařová M, Havlíčková V, Paul J, Ivánek R, Kuss AW, Hansíková H, Kaplanová V, et al. Tmem70 mutations cause isolated atp synthase deficiency and neonatal mitochondrial encephalocardiomyopathy. Nature genetics. 2008; 40(11):1288–1290. [PubMed: 18953340]

[23]. Mende S, Royer L, Herr A, Schmiedel J, Deschauer M, Klopstock T, Kostic VS, Schroeder M, Reichmann H, Storch A. Whole blood genome-wide expression profiling and network analysis suggest melas master regulators. Neurological research. 2011; 33(6):638–655. [PubMed: 21708074]

[24]. Ivanov VN, Ghandhi SA, Zhou H, Huang SX, Chai Y, Amundson SA, Hei TK. Radiation response and regulation of apoptosis induced by a combination of trail and chx in cells lacking mitochondrial dna: A role for nf-κb–stat3-directed gene expression. Experimental cell research. 2011; 317(11):1548–1566. [PubMed: 21440540]

[25]. Kovářová N, Čížková Vrbacká A, Pecina P, Stráneckỳ V, Pronicka E, Kmoch S, Houštěk J. Adaptation of respiratory chain biogenesis to cytochrome¡ i¿ c¡/i¿ oxidase deficiency caused by¡ i¿ surf1¡/i¿ gene mutations. Biochimica et Biophysica Acta (BBA)-Molecular Basis of Disease. 2012; 1822(7):1114–1124. [PubMed: 22465034]

[26]. Voets A, Huigsloot M, Lindsey P, Leenders A, Koopman W, Willems P, Rodenburg R, Smeitink J, Smeets H. Transcriptional changes in oxphos complex i deficiency are related to anti-oxidant pathways and could explain the disturbed calcium homeostasis. Biochimica et Biophysica Acta (BBA)-Molecular Basis of Disease. 2012; 1822(7):1161–1168. [PubMed: 22033105]

[27]. Chae S, Ahn BY, Byun K, Cho YM, Yu M-H, Lee B, Hwang D, Park KS. A systems approach for decoding mitochondrial retrograde signaling pathways. Science signaling. 2013; 6(264):rs4. [PubMed: 23443683]

[28]. Mormeneo E, Jimenez-Mallebrera C, Palomer X, De Nigris V, Vázquez-Carrera M, Orozco A, Nascimento A, Colomer J, Lerín C, Gómez-Foix AM. Pgc-1α induces mitochondrial and myokine transcriptional programs and lipid droplet and glycogen accumulation in cultured human skeletal muscle cells. PloS one. 2012; 7(1):e29985. [PubMed: 22272266]

[29]. Fernández-Ayala DJ, Guerra I, Jiménez-Gancedo S, Cascajo MV, Gavilán A, DiMauro S, Hirano M, Briones P, Artuch R, De Cabo R, et al. Survival transcriptome in the coenzyme q10 deficiency syndrome is acquired by epigenetic modifications: a modelling study for human coenzyme q10 deficiencies. BMJ open. 3(3)

[30]. Fernández-Ayala DJ, Guerra I, Jiménez-Gancedo S, Cascajo MV, Gavilán A, DiMauro S, Hirano M, Briones P, Artuch R, De Cabo R, et al. Survival transcriptome in the coenzyme q10 deficiency

syndrome is acquired by epigenetic modifications: a modelling study for human coenzyme q10 deficiencies. BMJ open. 3(3)

[31]. Cabeza-Arvelaiz Y, Schiestl RH. Transcriptome analysis of a rotenone model of parkinsonism reveals complex i-tied and-untied toxicity mechanisms common to neurodegenerative diseases. PloS one. 2012; 7(9):e44700. [PubMed: 22970289]

[32]. Falk M, Zhang Z, Rosenjack J, Nissim I, Daikhin E, Nissim I, Sedensky M, Yudkoff M, Morgan P. Metabolic pathway profiling of mitochondrial respiratory chain mutants in¡ i¿ c. elegans¡/i¿. Molecular genetics and metabolism. 2008; 93(4):388–397. [PubMed: 18178500]

[33]. Calvo S, Jain M, Xie X, Sheth SA, Chang B, Goldberger OA, Spinazzola A, Zeviani M, Carr SA, Mootha VK. Systematic identification of human mitochondrial disease genes through integrative genomics. Nature genetics. 2006; 38(5):576–582. [PubMed: 16582907]

[34]. Someya S, Yamasoba T, Kujoth GC, Pugh TD, Weindruch R, Tanokura M, Prolla TA. The role of mtdna mutations in the pathogenesis of age-related hearing loss in mice carrying a mutator dna polymerase γ. Neurobiology of aging. 2008; 29(7):1080–1092. [PubMed: 17363114]

[35]. Cunningham JT, Rodgers JT, Arlow DH, Vazquez F, Mootha VK, Puigserver P. mtor controls mitochondrial oxidative function through a yy1–pgc-1&agr; transcriptional complex. nature. 2007; 450(7170):736–740. [PubMed: 18046414]

[36]. Cui L, Jeong H, Borovecki F, Parkhurst CN, Tanese N, Krainc D. Transcriptional repression of pgc-1α by mutant huntingtin leads to mitochondrial dysfunction and neurodegeneration. Cell. 2006; 127(1):59–69. [PubMed: 17018277]

[37]. Vianna CR, Huntgeburth M, Coppari R, Choi CS, Lin J, Krauss S, Barbatelli G, Tzameli I, Kim Y-B, Cinti S, et al. Hypomorphic mutation of pgc-1β causes mitochondrial dysfunction and liver insulin resistance. Cell metabolism. 2006; 4(6):453–464. [PubMed: 17141629]

[38]. Peng M, Falk MJ, Haase VH, King R, Polyak E, Selak M, Yudkoff M, Hancock WW, Meade R, Saiki R, et al. Primary coenzyme q deficiency in pdss2 mutant mice causes isolated renal disease. PLoS genetics. 2008; 4(4):e1000061. [PubMed: 18437205]

[39]. Moisoi N, Klupsch K, Fedele V, East P, Sharma S, Renton A, Plun-Favreau H, Edwards R, Teismann P, Esposti M, et al. Mitochondrial dysfunction triggered by loss of htra2 results in the activation of a brain-specific transcriptional stress response. Cell Death & Differentiation. 2009; 16(3):449–464. [PubMed: 19023330]

[40]. Zhang Z, Gasser DL, Rappaport EF, Falk MJ. Cross-platform expression microarray performance in a mouse model of mitochondrial disease therapy. Molecular genetics and metabolism. 2010; 99(3):309–318. [PubMed: 19944634]

[41]. Finley LW, Carracedo A, Lee J, Souza A, Egia A, Zhang J, Teruya-Feldstein J, Moreira PI, Cardoso SM, Clish CB, et al. Sirt3 opposes reprogramming of cancer cell metabolism through hif1α destabilization. Cancer cell. 2011; 19(3):416–428. [PubMed: 21397863]

[42]. Falk MJ, Polyak E, Zhang Z, Peng M, King R, Maltzman JS, Okwuego E, Horyn O, Nakamaru-Ogiso E, Ostrovsky J, et al. Probucol ameliorates renal and metabolic sequelae of primary coq deficiency in pdss2 mutant mice. EMBO molecular medicine. 2011; 3(7):410–427. [PubMed: 21567994]

[43]. Hirschey MD, Shimazu T, Jing E, Grueter CA, Collins AM, Aouizerat B, Stančáková A, Goetzman E, Lam MM, Schwer B, et al. Sirt3 deficiency and mitochondrial protein hyperacetylation accelerate the development of the metabolic syndrome. Molecular cell. 2011; 44(2):177–190. [PubMed: 21856199]

[44]. Finley LW, Lee J, Souza A, Desquiret-Dumas V, Bullock K, Rowe GC, Procaccio V, Clish CB, Arany Z, Haigis MC. Skeletal muscle transcriptional coactivator pgc-1α mediates mitochondrial, but not metabolic, changes during calorie restriction. Proceedings of the National Academy of Sciences. 2012; 109(8):2931–2936.

[45]. Wheeler DL, Barrett T, Benson DA, Bryant SH, Canese K, Chetvernin V, Church DM, DiCuccio M, Edgar R, Federhen S, et al. Database resources of the national center for biotechnology information. Nucleic acids research. 2007; 35(suppl 1):D5–D12. [PubMed: 17170002]

[46]. Irizarry RA, Bolstad BM, Collin F, Cope LM, Hobbs B, Speed TP. Summaries of affymetrix genechip probe level data. Nucleic acids research. 2003; 31(4):e15–e15. [PubMed: 12582260]

[47]. Dai M, Wang P, Boyd AD, Kostov G, Athey B, Jones EG, Bunney WE, Myers RM, Speed TP, Akil H, et al. Evolving gene/transcript definitions significantly alter the interpretation of genechip data. Nucleic acids research. 2005; 33(20):e175–e175. [PubMed: 16284200]

[48]. Fisher, RA. Statistical methods for research workers. Genesis Publishing Pvt Ltd; 1925.

[49]. Cheng Y, Church GM. Biclustering of expression data. Ismb. 2000; 8:93–103. [PubMed: 10977070]

[50]. Ben-Dor A, Chor B, Karp R, Yakhini Z. Discovering local structure in gene expression data: the order-preserving submatrix problem. Journal of computational biology. 2003; 10(3-4):373–384. [PubMed: 12935334]

[51]. Barkow S, Bleuler S, Prelić A, Zimmermann P, Zitzler E. Bicat: a biclustering analysis toolbox. Bioinformatics. 2006; 22(10):1282–1283. [PubMed: 16551664]

[52]. Dennis G Jr, Sherman BT, Hosack DA, Yang J, Gao W, Lane HC, Lempicki RA, et al. David: database for annotation, visualization, and integrated discovery. Genome biol. 2003; 4(5):P3. [PubMed: 12734009]

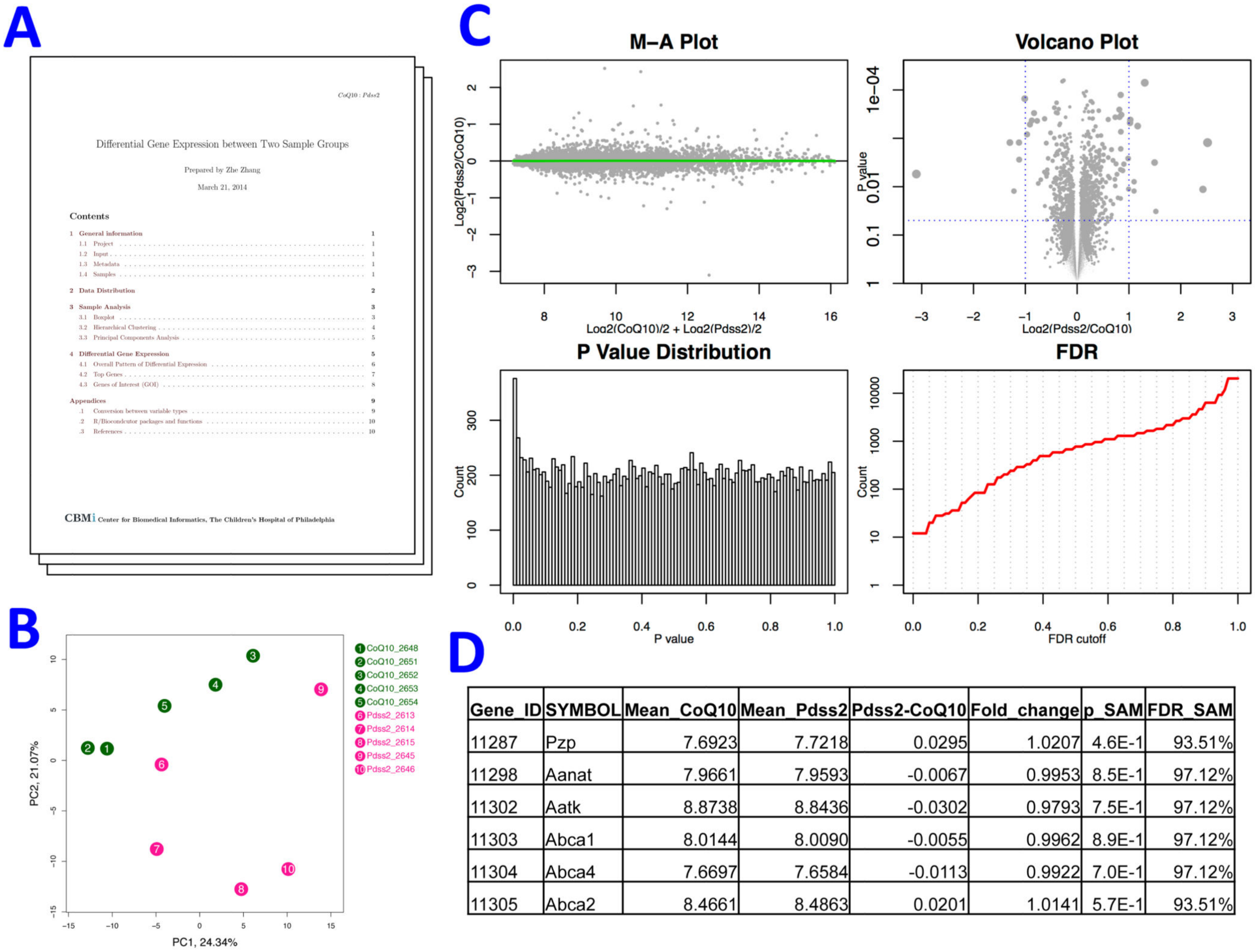

CoQ10 : Pdss2

Differential Gene Expression between Two Sample Groups

Prepared by Zhe Zhang

March 21, 2014

Contents

CBMi Center for Biomedical Informatics, The Children's Hospital of Philadelphia

Gene_ID	SYMBOL	Mean_CoQ10	Mean_Pdss2	Pdss2-CoQ10	Fold_change	p_SAM	FDR_SAM
11287	Pzp	7.6923	7.7218	0.0295	1.0207	4.6E-1	93.51%
11298	Aanat	7.9661	7.9593	-0.0067	0.9953	8.5E-1	97.12%
11302	Aatk	8.8738	8.8436	-0.0302	0.9793	7.5E-1	97.12%
11303	Abca1	8.0144	8.0090	-0.0055	0.9962	8.9E-1	97.12%
11304	Abca4	7.6697	7.6584	-0.0113	0.9922	7.0E-1	97.12%
11305	Abca2	8.4661	8.4863	0.0201	1.0141	5.7E-1	93.51%

Figure 1.

Synopsis of a pairwise comparison. The standardized outputs of a pairwise comparison of transcriptomes of two sample groups included a report file and a set of figures and tables. A) A report in PDF format that summarized data quality and comparison results. B) Unsupervised clustering of compared samples via principal components analysis. C) Visualization of comparison results. M-A plot evaluates dependence of group difference on baseline levels of gene expression. Volcano plot illustrates both magnitude (x-axis) and statistical significance (y-axis) of differential expression. P value distribution should be skewed to the left side when the comparison identifies a difference of expression profiles between two groups, and the FDR plot shows the number of genes with FDR lower than a given value. D) Full table of comparison results and DAVID functional analysis based on these results (not shown) were written to an Excel file.

Genes	COX5B, COX8A, NDUFA9, SUCLG1, UQCRQ	
Samples	**Sample**	**Dataset**
	Patient_CoQ_MELQ1	H_dataset11
	Patient_CoQ_SOFQ1	H_dataset11
	Patient_ELO21	H_dataset11
	X0nM_1W_2	H_dataset12
	Patient_9	H_dataset2
	Patient_5	H_dataset2
	P11	H_dataset3
	P7	H_dataset3
	P8	H_dataset3
	Patient_6613_Glucose	H_dataset7
	Patient_5175_Glucose	H_dataset7
	WT_rep1_norm1	H_dataset8
	Het_rep1_norm1	H_dataset8

(a) Human dataset bicluster 3 genes and samples. The samples part shows every sample that involved in the bicluster and the source dataset for that sample.

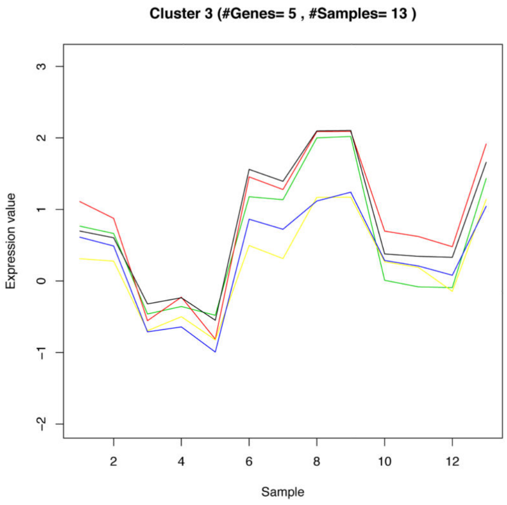

(b) Expression data of human dataset bicluster 3. Each line shows a gene from the bicluster across the samples.

Figure 2.

Human dataset bicluster 3.

Genes	Allc, Fgr, P2rx1, Trpm1, Wdr4	
Samples	**Sample**	**Dataset**
	Day3_PGC1a_3	M_dataset1
	Day3_PGC1a_2	M_dataset1
	Day3_GFP_1	M_dataset1
	KO_Control_10	M_dataset12
	WT_Control_4	M_dataset12
	WT_Control_5	M_dataset12
	KO2	M_dataset4
	WT2	M_dataset4
	Muscle_Control_3	M_dataset5
	Liver_Control_1	M_dataset5
	WT_Con_3	M_dataset7
	WT_Rot_3	M_dataset7
	WT_Con_1	M_dataset7
	KO_Con_2	M_dataset7
	WT_Con_2	M_dataset7

(a) Mouse dataset bicluster 3 genes and samples. The samples part shows every sample that involved in the bicluster and the source dataset for that sample.

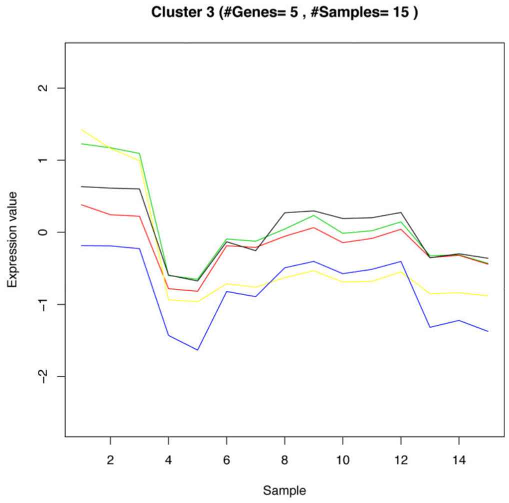

(b) Expression data of mouse dataset bicluster 3. Each line shows a gene from the bicluster across the samples.

Figure 3.

Mouse dataset bicluster 3.

	Sample	Dataset
Genes	CELE_F54D10.5, C01G5.6, sas-5, B0464.9, C48B4.11	
Samples	MT_5	W_dataset1
	WT_4	W_dataset1
	WT_1	W_dataset1
	MT_I_RNAi_5	W_dataset2
	MT_I_RNAi_4	W_dataset2
	MT_I_Mis	W_dataset2
	WT_Mis	W_dataset2
	MT_III_Mis	W_dataset2
	WT_RNAi	W_dataset2
	MT_I_RNAi_1	W_dataset2
	DMSO_20D_2	W_dataset3
	Rotenone_20D_2	W_dataset3
	DMSO_10D_2	W_dataset3
	DMSO_5D_1	W_dataset3
	Rotenone_5D_1	W_dataset3
	Rotenone_5D_3	W_dataset3
	DMSO_10D_1	W_dataset3

(a) Worm dataset bicluster 3 genes and samples. The samples part shows every sample that involved in the bicluster and the source dataset for that sample.

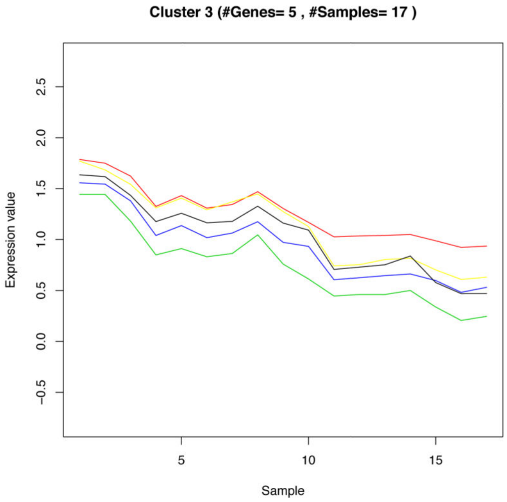

(b) Expression data of worm dataset bicluster 3. Each line shows a gene from the bicluster across the samples.

Figure 4.

Worm dataset bicluster 3.

Genes	CG2972, CG32344, kz, Mt2, mtSSB, Nop56, Rtc1	
Samples	**Sample**	**Dataset**
	X	F_dataset1
	KO_M_2	F_dataset1
	WT_F_1	F_dataset1
	WT_M_2	F_dataset1
	WT_M_3	F_dataset1
	Ex3_GFP_72	F_dataset2
	Ex2_COVa_168	F_dataset2
	Ex1_GFP_48	F_dataset2
	Ex1_GFP_168	F_dataset2
	Ex2_GFP_168	F_dataset2
	Ex2_GFP_120	F_dataset2
	Ex2_COVa_96	F_dataset2
	Ex2_GFP_96	F_dataset2
	Ex3_CoVa_120	F_dataset2
	Ex3_CoVa_96	F_dataset2
	Ex3_GFP_96	F_dataset2

(a) Fly dataset bicluster 3 genes and samples. The samples part shows every sample that involved in the bicluster and the source dataset for that sample.

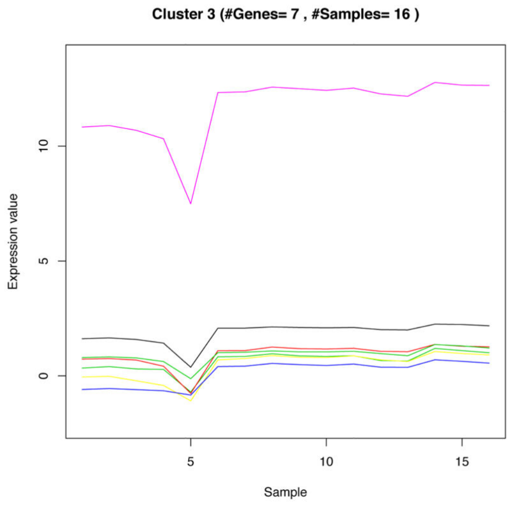

(b) Expression data of fly dataset bicluster 3. Each line shows a gene from the bicluster across the samples.

Figure 5.
Fly dataset bicluster 3.

Table 1

The four living species datasets description.

Species[a]	DS Id[b]	GEO_ID[c]	Ref.[d]	Tissue[e]	#Samples[f]	#Genes[g]	#Groups (classes)[h]
Fly	F_dataset1	GSE10169	[15]	Whole body	12	12,522	4
	F_dataset2	GSE32912	[16]	S2 cell	21	12,522	11
Worm	W_dataset1	GSE9896	[17]	Whole body	10	16,812	2
	W_dataset2	GSE9897	[18]	Whole body	10	16,812	6
	W_dataset3	GSE46051	[19]	Whole body	22	28,355	8
Human	H_dataset1	GSE1462	[20]	Skeletal muscle	15	12,027	4
	H_dataset2	GSE8648	[21]	Fibroblast	22	1,190	2
	H_dataset3	GSE10956	[22]	Fibroblast	22	13,031	2
	H_dataset4	GSE14882	[23]	Peripheral blood	16	12,027	2
	H_dataset5	GSE24945[i]	[24]	Fibroblast	12	19,617	4
	H_dataset6	GSE26322	[25]	Fibroblast	12	19,063	2
	H_dataset7	GSE27041	[26]	Fibroblast	20	18,895	4
	H_dataset8	GSE27545	[27]	Cybrid	17	19,600	6
	H_dataset9	GSE28206	[28]	Skeletal muscle	7	19,600	2
	H_dataset10	GSE33769	[29]	Fibroblast	15	18,895	2
	H_dataset11	GSE33940	[30]	Fibroblast	20	19,714	3
	H_dataset12	GSE35642	[31]	SK-N-MC cell	18	12,027	6
	H_dataset13	GSE42986	[32]	Muscle/FCL	40	20,708	4
Mouse	M_dataset1	GSE4330	[33]	Myoblast (C2C12)	21	14,706	7
	M_dataset2	GSE4866	[34]	Cochlea	10	17,480	2
	M_dataset3	GSE5332	[35]	MEF	13	17,480	4
	M_dataset4	GSE5786	[36]	Striata	6	20,628	2
	M_dataset5	GSE6210	[37]	Liver/Muscle	12	17,480	4
	M_dataset6	GSE10904	[38]	Liver	6	17,480	2
	M_dataset7	GSE13034	[39]	MEF	14	12,279	4
	M_dataset8	GSE18677[i]	[40]	Liver	11	17,480	8
	M_dataset9	GSE27309	[41]	Brown adipose	20	20,299	2
	M_dataset10	GSE27954	[42]	Liver	12	21,154	4
	M_dataset11	GSE30552	[43]	Liver	26	17,480	4
	M_dataset12	GSE34773	[44]	Skeletal muscle	26	17,480	4

[a] The dataset species.

[b] DS Id is the dataset id number that is used in this study.

[c] The GEO_ID in the NCBI database.

[d] The dataset reference.

[e] The tissue that the sample comes from.

[f] The number of samples in the dataset.

[g] The number of genes in the dataset.

[h] The number of sample groups in the dataset.

[i] Too many missing values in this dataset.

Table 2

Species datasets overlap and the extracted bicluster results summary.

Overlap	Species[a]	#Genes[b]	#Samples[c]	#Biclusters[d]	Avg MSR_x[e]
Single [f]	F	12,521	33	5	0.87
	M	10,279	147	5	0.92
	H	895	233	6	0.93
	W	16,688	42	6	0.98
Pairwise [g]	F,H	443	256	8	0.87
	H,W	377	265	6	0.80
	M,H	675	370	1	0.99
	F,W	2,724	75	9	**0.96** [j]
	F,M	2,944	180	7	**0.95** [j]
	W,M	2,240	189	8	0.88
Triplet [h]	F,W,M	1,637	222	7	**0.92** [j]
	H,F,M	341	403	0[k]	–
	H,W,F	307	298	0[k]	–
	H,W,M	286	412	0[k]	–
All [i]	H,F,M,W	235	445	7	0.85

[a] F: Fly; W: Worm; M: Mouse; H: Human.

[b] The number of genes in the dataset.

[c] The number of samples in the dataset.

[d] Number of biclusters with gene counts and sample counts more than or equal5.

[e] The average mean squared residue of for the chosen biclusters with gene counts and sample counts more than or equal 5.

[f] The overlap of the datasets in each living species.

[g] The overlap of the species datasets in pairs.

[h] The overlap of the species datasets in triplets.

[i] The overlap across all species.

[j] The best MSR results in the overlapped datasets.

[k] All of the extracted biclusters gene counts or sample counts less than 5.

Table 3

The DAVID terms identified by multiple pairwise comparisons. DAVID analysis was performed on differentially expressed genes identified by each pairwise comparison. Terms enriched within these genes with FDR less than 0.05 were summarized across all 60 comparisons. This table listed some of terms most commonly identified by multiple comparisons.

Term	ID	Num Comparisons[a]	Num Dataset[b]	Num Species[c]
Mitochondrion	GO:0005739	21	14	3
Oxidation reduction	GO:0055114	20	12	3
Generation of precursor metabolites and energy	GO:0006091	13	9	3
Electron transport chain	GO:0022900	12	9	3
Biological adhesion	GO:0022610	12	10	3
Ribonucleoprotein complex	GO:0030529	10	9	3
Skeletal system development	GO:0001501	10	6	3

[a] The number of comparisons (*total* = 60);

[b] Data sets (*total* = 28);

[c] Species (*total* = 4) within which the term was identified with FDR < 0.05.

Table 4

The homolog gene clusters identified by multiple pairwise comparisons. Genes of different species were mapped to homolog cluster for summarization across comparisons. Top 2% genes with the most significant p values were selected from each comparison. Poisson test (λ = 0.02) was performed on each gene cluster to identify those gene clusters more likely to be included in the top 2% lists. This table listed the most significant clusters identified by at least 5 independent data sets generated from at least 3 species.

Homolog ID	Human Gene	Human Symbol	Num Total[a]	Num Comparison[b]	Num Dataset[b]	Num Species[b]	p Poisson	FDR Poisson
8622	23474	ETHE1	60	12	7	4	6.17E-09	6.31E-05
55759	8140	SLC7A5	52	11	5	3	1.49E-08	9.21E-05
3343	4716	NDUFB10	52	9	6	3	1.55E-06	4.51E-03
1547	2617	GARS	60	9	5	3	4.86E-06	6.72E-03
2255	6390	SDHB	60	9	7	3	4.86E-06	6.72E-03
37514	513	ATP5D	60	9	7	4	4.86E-06	6.72E-03
4788	10667	FARS2	55	8	5	3	2.01E-05	1.21E-02
68163	290	ANPEP	55	8	5	3	2.01E-05	1.21E-02
3	34	ACADM	60	8	6	3	3.70E-05	1.68E-02
3356	5106	PCK2	60	8	6	3	3.70E-05	1.68E-02
457	6609	SMPD1	60	8	5	3	3.70E-05	1.68E-02
55662	4967	OGDH	60	8	7	3	3.70E-05	1.68E-02
10884	4729	NDUFV2	45	7	5	3	4.34E-05	1.93E-02

[a] The total number of comparisons that included this gene cluster;

[b] Num_Comparison, Num_Dataset, and Num_Species: the number of comparisons, data sets, and species that identified this cluster within the top 2% lists

Table 5

The pairwise comparisons correlated to each other. Fold changes of two pairwise comparisons were used to calculate a correlation coefficient. This table listed pairs of the comparisons from different data sets or species having the strongest correlation to each other.

Comparison1	Dataset1	Species1	Comparison2	Dataset2	Species2	N[a]	Corr[b]
50nM Rotenone, 1 week	GSE35642	human	Mito patients muscle	GSE42986	human	11472	−0.42
5nM Rotenone, 4 weeks	GSE35642	human	Mito patients muscle	GSE42986	human	11472	0.39
Patients with CoQ10 def.	GSE33940	human	Mito patients muscle	GSE42986	human	17453	0.37
Sirt3 KO, standard diet	GSE30552	mouse	Mito patients muscle	GSE42986	human	16139	−0.37
Sirt3 KO, standard diet	GSE30552	mouse	Probucol treatment	GSE18677	mouse	16692	−0.35
Patients of 4977bp del	GSE1462	human	Mito patients muscle	GSE42986	human	11472	0.34
PGC1b KO in liver	GSE6210	mouse	Rotenone, 1 day old	GSE46051	worm	3153	0.32
PGC1a overexpression	GSE4330	mouse	PGC1a KO, standard diet	GSE34773	mouse	12941	−0.30

[a] Number of homolog gene clusters included by both comparisons;

[b] Pearson’s correlation coefficient between 2 sets of fold changes.

Table 6

Filtered human biclusters details.

Bicluster#[a]	**#Genes**[b]	**#Samples**[c]	***MSR_x***[d]	**Enriched%**[e]
3	5	13	**0.9678**[f]	100
4	7	11	0.9576	100
5	11	10	0.9388	100
6	17	9	0.9294	100
7	26	8	0.8975	100
8	49	7	0.8791	100

[a] The bicluster serial number in this study.

[b] The number of genes involved in the bicluster.

[c] The number of samples involved in the bicluster.

[d] The bicluster coherence that explained in section 2.6.6.

[e] The percent of enriched genes from the bicluster (*# enriched genes / total number of genes*.)

[f] The best MSR_X score is 0.9678.

Table 7

Sample of the enrichment analysis results. Enrichment analysis results for the highest human dataset $MSR_{\mathcal{X}}$ bicluster, bicluster 3, using DAVID tools.

Category[a]	Term[b]	Genes[c]	%[d]	P–Value	Fisher Exact
SP_PIR_KEYWORDS	respiratory chain	NDUFA9, COX8A, UQCRQ, COX5B	80	1.90E-07	8.50E-10
GOTERM_CC_FAT	mitochondrial inner membrane	NDUFA9, SUCLG1, COX8A, UQCRQ, COX5B	100	3.20E-07	7.60E-09
GOTERM_CC_FAT	organelle inner membrane	NDUFA9, SUCLG1, COX8A, UQCRQ, COX5B	100	4.30E-07	1.10E-08
GOTERM_CC_FAT	mitochondrial membrane	NDUFA9, SUCLG1, COX8A, UQCRQ, COX5B	100	8.90E-07	2.70E-08
GOTERM_CC_FAT	mitochondrial envelope	NDUFA9, SUCLG1, COX8A, UQCRQ, COX5B	100	1.10E-06	3.70E-08
SP_PIR_KEYWORDS	mitochondrion	NDUFA9, SUCLG1, COX8A, UQCRQ, COX5B	100	3.50E-06	1.50E-07
GOTERM_CC_FAT	mitochondrial part	NDUFA9, SUCLG1, COX8A, UQCRQ, COX5B	100	4.70E-06	2.20E-07
GOTERM_CC_FAT	organelle envelope	NDUFA9, SUCLG1, COX8A, UQCRQ, COX5B	100	5.50E-06	2.60E-07
GOTERM_CC_FAT	envelope	NDUFA9, SUCLG1, COX8A, UQCRQ, COX5B	100	5.60E-06	2.70E-07
GOTERM_BP_FAT	generation of precursor metabolites and energy	NDUFA9, SUCLG1, COX8A, UQCRQ	80	4.80E-05	1.40E-06
GOTERM_CC_FAT	mitochondrion	NDUFA9, SUCLG1, COX8A, UQCRQ, COX5B	100	5.20E-05	4.40E-06
GOTERM_CC_FAT	organelle membrane	NDUFA9, SUCLG1, COX8A, UQCRQ, COX5B	100	5.40E-05	4.60E-06
UP_SEQ_FEATURE	transit peptide:Mitochondrion	NDUFA9, SUCLG1, COX8A, COX5B	80	5.70E-05	1.70E-06
SP_PIR_KEYWORDS	transit peptide	NDUFA9, SUCLG1, COX8A, COX5B	80	5.90E-05	1.80E-06
KEGG_PATHWAY	Parkinson’s disease	NDUFA9, COX8A, UQCRQ, COX5B	80	6.10E-05	1.90E-06
KEGG_PATHWAY	Oxidative phosphorylation	NDUFA9, COX8A, UQCRQ, COX5B	80	6.40E-05	2.00E-06
KEGG_PATHWAY	Alzheimer’s disease	NDUFA9, COX8A, UQCRQ, COX5B	80	1.30E-04	5.00E-06
KEGG_PATHWAY	Huntington’s disease	NDUFA9, COX8A, UQCRQ, COX5B	80	1.70E-04	7.40E-06
GOTERM_MF_FAT	hydrogen ion transmembrane transporter activity	COX8A, UQCRQ, COX5B	60	2.80E-04	3.20E-06
GOTERM_MF_FAT	monovalent inorganic cation transmembrane transporter activity	COX8A, UQCRQ, COX5B	60	3.80E-04	4.90E-06

Category[a]	Term[b]	Genes[c]	%[d]	P–Value	Fisher Exact
SP_PIR_KEYWORDS	mitochondrion inner membrane	COX8A, UQCRQ, COX5B	60	5.90E-04	9.80E-06
GOTERM_MF_FAT	inorganic cation transmembrane transporter activity	COX8A, UQCRQ, COX5B	60	7.90E-04	1.50E-05
KEGG_PATHWAY	Cardiac muscle contraction	COX8A, UQCRQ, COX5B	60	1.40E-03	3.40E-05
SP_PIR_KEYWORDS	mitochondrial inner membrane	COX8A, COX5B	40	3.90E-03	9.20E-06
SP_PIR_KEYWORDS	oxidoreductase	NDUFA9, COX8A, COX5B	60	4.90E-03	2.40E-04
SP_PIR_KEYWORDS	membrane-associated complex	COX8A, COX5B	40	6.60E-03	2.70E-05
SP_PIR_KEYWORDS	oxidative phosphorylation	COX8A, COX5B	40	7.30E-03	3.20E-05
GOTERM_MF_FAT	oxidoreductase activity, acting on heme group of donors	COX8A, COX5B	40	8.60E-03	4.50E-05
GOTERM_MF_FAT	cytochrome-c oxidase activity	COX8A, COX5B	40	8.60E-03	4.50E-05
GOTERM_MF_FAT	heme-copper terminal oxidase activity	COX8A, COX5B	40	8.60E-03	4.50E-05
GOTERM_MF_FAT	oxidoreductase activity, acting on heme group of donors, oxygen as acceptor	COX8A, COX5B	40	8.60E-03	4.50E-05
SP_PIR_KEYWORDS	electron transfer	COX8A, COX5B	40	1.00E-02	6.60E-05
SP_PIR_KEYWORDS	electron transport	NDUFA9, UQCRQ	40	2.10E-02	2.60E-04
GOTERM_CC_FAT	respiratory chain	NDUFA9, UQCRQ	40	2.30E-02	3.40E-04
GOTERM_BP_FAT	cellular respiration	NDUFA9, SUCLG1	40	2.80E-02	5.00E-04
GOTERM_BP_FAT	electron transport chain	NDUFA9, UQCRQ	40	3.30E-02	6.90E-04
INTERPRO	NAD(P)-binding domain	NDUFA9, SUCLG1	40	3.60E-02	7.90E-04
UP_SEQ_FEATURE	cross-link:Glycyl lysine isopeptide (Lys-Gly) (interchain with G-Cter in ubiquitin)	SUCLG1, UQCRQ	40	4.10E-02	1.10E-03
GOTERM_BP_FAT	energy derivation by oxidation of organic compounds	NDUFA9, SUCLG1	40	4.20E-02	1.10E-03
SP_PIR_KEYWORDS	isopeptide bond	SUCLG1, UQCRQ	40	6.50E-02	2.70E-03
GOTERM_CC_FAT	mitochondrial lumen	NDUFA9, SUCLG1	40	6.90E-02	3.00E-03
GOTERM_CC_FAT	mitochondrial matrix	NDUFA9, SUCLG1	40	6.90E-02	3.00E-03
SP_PIR_KEYWORDS	acetylation	NDUFA9, SUCLG1, COX5B	60	9.30E-02	2.10E-02

[a] The original source (i.e., database) of the term.

[b] The enrichment terms associated with the gene list.

[c] The list of genes from the bicluster that is involved in the term.

[d] The percentage of the bicluster genes that involved in this term (*Involved genes/total genes*).

Table 8

Filtered mouse biclusters details.

Bicluster#[a]	**#Genes**[b]	**#Samples**[c]	$\boldsymbol{MSR_x}$ [d]	**Enriched%**[e]
3	5	15	**0.9471** [f]	40
4	6	13	0.9228	33.3
5	10	12	0.9362	70
6	19	11	0.8810	63.2
7	43	10	0.9070	86

[a] The bicluster serial number in this study.

[b] The number of genes involved in the bicluster.

[c] The number of samples involved in the bicluster.

[d] The bicluster coherence that explained in section 2.6.6.

[e] The percent of enriched genes from the bicluster (*# enriched genes / total number of genes*.)

[f] The best MSR_X score is 0.9471.

Table 9

Filtered worm biclusters details.

Bicluster#[a]	**#Genes**[b]	**#Samples**[c]	$\boldsymbol{MSR_x}$ [d]	**Enriched%**[e]
3[a]	5	17	**0.9969** [f]	0
4[a]	9	16	0.9820	0
5	15	15	0.9804	46.7
6	37	14	0.9767	64.9
7	43	13	0.9693	58.1
8	112	12	0.9736	64.3

[a] The bicluster serial number in this study.

[b] The number of genes involved in the bicluster.

[c] The number of samples involved in the bicluster.

[d] The bicluster coherence that explained in section 2.6.6.

[e] The percent of enriched genes from the bicluster (*# enriched genes / total number of genes*.)

[f] The best MSR_X score is 0.9969.

Table 10

Filtered fly biclusters details.

Bicluster#[a]	#Genes[b]	#Samples[c]	MSR_x [d]	Enriched%[e]
3	7	16	**0.8875** [f]	85
4	9	15	0.8634	77.8
5	20	14	0.8619	75
6	33	13	0.8801	78.8
7	70	12	0.8691	72.9

[a] The bicluster serial number in this study.

[b] The number of genes involved in the bicluster.

[c] The number of samples involved in the bicluster.

[d] The bicluster coherence that explained in section 2.6.6.

[e] The percent of enriched genes from the bicluster (*# enriched genes / total number of genes.*)

[f] The best MSR_X score is 0.8875.